ON THE GEOMETRY DESIGN OF ALN LAMB WAVE RESONATORS WITH PREDEFINED SHALLOW RELEASE CAVITIES

Tzu-Hsuan Hsu[1], Guan-Lin Wu[1], Yan-Ming Huang[1], Yens Ho[2], Yung-Hsiang Chen[2], Yelehanka Pradeep[3], Rakesh Chand[3], and Ming-Huang Li[1]*
[1]National Tsing Hua University, Hsinchu, Taiwan
[2]Vanguard International Semiconductor Corporation, Hsinchu, Taiwan
[3]Vanguard International Semiconductor Corporation Singapore PTE. Ltd., Singapore

ABSTRACT

In this work, we demonstrate a 700 MHz one-port aluminum nitride (AlN) S_0-mode *residual stress-resilient* Lamb wave resonator (LWR) with lithographically defined acoustic boundaries based on a CMOS-compatible 8-inch MEMS process, exhibiting a high-quality factor (Q) of 2,422 and an electromechanical coupling factor (k_{eff}^2) of 1.05%. Although a well-defined shallow "etch sandbox" provides a higher quality factor and better mechanical robustness to the LWR over conventional isotropic silicon etching processes, the performance of the LWR becomes sensitive to the deformation caused by residual stress in the thin films. In this work, with the assistance of laser scanning confocal microscopy, the physical contact between deformed LWR and the bottom of the cavity is identified as a new failure mode. We investigate three LWRs with different aspect ratios and anchors, revealing that the width of the anchors is the key to suppressing out-of-plane deformations. The residual stress-resilient wide-anchor LWR shows a promising f-Q product of 1.69×10^{12} and $k_{\text{eff}}^2 > 1.05\%$, which is comparable with that of state-of-the-art AlN LWRs.

KEYWORDS

High-Q, S_0-mode, Lamb Wave Resonator, Residual Stress.

INTRODUCTION

Radio frequency front-end (RFFE) has become a key building block within modern day wireless communication systems, serving as a crucial component in signal processing application. Device based on AlN technology has dominated the market in the past decades as it offers high phase velocity, CMOS compatibility, great manufacturability, and reliability [1]. Among various technologies used to realize acoustic devices in AlN, LWR has attracted much research attention as it inherited the multi-frequency flexibility of surface acoustic wave (SAW) devices while significantly shrank the overall footprint of the device. Although Bulk acoustic wave (BAW) resonators also provide such benefit, it is very challenging to achieve multi-frequency operation in a single chip. Hence, LWR devices can be seen as a promising candidate eyeing for a highly compact and integrated RFFE. Which is getting ever important in modern RFFE design since more and more functions and frequency bands are allocated in one single module. For instance, high frequency reference signal can simply be implemented on the same chip using LWR-based oscillators.

Comparing with other Lamb wave mode realized in AlN, fundamental symmetric (S_0) LWR has become popular research topic [2] as it offers high quality factor (Q) and moderate k_{eff}^2. The operation frequency of S_0 LWR can also be determined by the phase velocity and wavelength based on the excited S_0 wave. Moreover, since the acoustic energy is confined within the suspended plate, there are less energy loss in S_0 LWR. The suspended structure can simply be created by substrate removal. More specifically, to release and undercut the device, frontside isotropic substrate release is typically preferred. However, this approach releases both the device and unwanted undercuts below anchors or supporting tethers (As

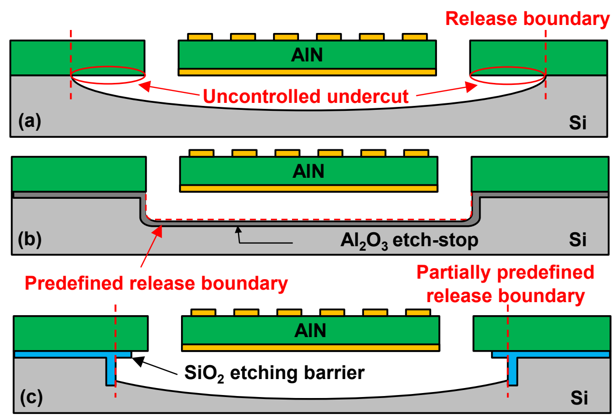

Figure 1. Comparison of three different release process to achieve suspended LWR without double side alignment and backside etching. (a) substrate isotropic etch [3]; (b) "release sandbox" [5][6]; (c) Etching barrier [7].

shown in Fig. 1(a) [3]). Although precise time control may help reducing this matter, it is impossible to achieve a precisely defined acoustic boundary. Prior studies have shown that energy loss caused by undercut in LWR is a key factor limiting their Q factor performance [4]. Therefore, several methods were proposed to define a precise acoustic boundary. By generating a predefined "release sandbox" enclosed by a etch-stop layer (as shown in Fig. 1(b)), it is possible to form a precisely defined acoustic boundary for Q enhancement [5][6]. Other technique such as introducing an etching barrier (as shown in Fig. 1(c)) has also been proposed [7] to partially predefine the release boundary. These techniques have all been proven to have positive effect towards achieving high Q in S_0 LWR.

Therefore, in this work, we proposed such a S_0 LWR based on a shallow release trench approach. By specifically designed to operate at higher frequency as compared with previously published results [3,5-7], the correlation between release boundary and Q is again verified with shorter wavelength S_0 wave. Through different geometry designs, LWR with residual stress resilient design was successfully demonstrated. By identifying the unique failure mode for devices based on shallow release cavity, there are great potentials in mass fabrication of high Q LWR if the resonator avoids physical contact with the release cavity. By further incorporating techniques such as scandium (Sc)-doping [9], k_{eff}^2 comparable or higher than current BAW devices can also be achieved, making LWR a strong alternative for the next-generation highly integrated RFFE.

DEVICE DESIGN AND FABRICATION

The proposed S_0 LWR was fabricated in an 8-inch CMOS compatible MEMS foundry. To obtain the "release sandbox" feature,

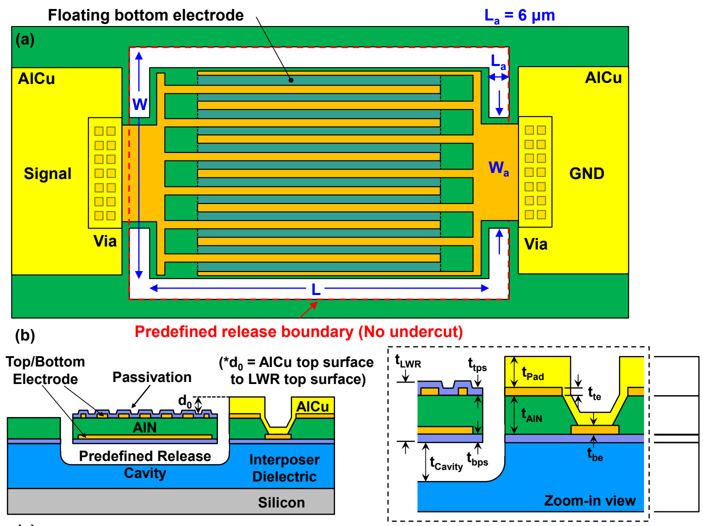

#	Symbol	Layer	Thickness	#	Symbol	Layer	Thickness
1	$t_{Pad} = d_0$	Pad (AlCu)	1000 nm	5	t_{be}	Bottom elec. (Mo)	250 nm
2	t_{tps}	Top passivation	200 nm	6	t_{bps}	Bottom passivation	100 nm
3	t_{te}	Top elec. (Mo)	250 nm	7	t_{Cavity}	Predefined cavity	8~900 nm
4	t_{AlN}	Device layer (AlN)	1000 nm	8	t_{LWR}	Total LWR thickness	1800 nm

Figure 2. Mock-up view of the proposed S_0 LWR (a) top-view (b) cross-sectional view and (c) the dimensions for the acoustic resonator's design parameters.

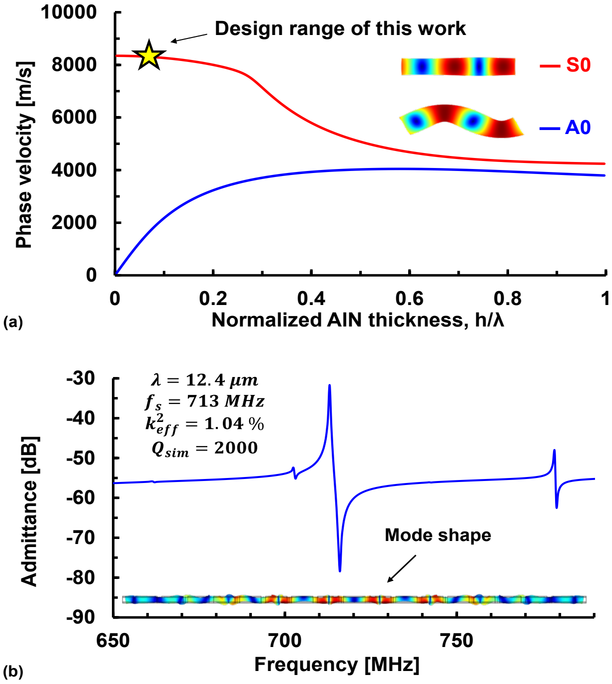

Figure 3. FEA simulation of the proposed resonator: (a) phase velocity dispersion of a 1 µm-thick AlN slab with thick (250 nm) Mo electrodes; (b) admittance magnitude of the proposed S_0 LWR.

an interposer dielectric layer was first deposited atop the handling Si wafer followed by etching of interposer to create cavity and refilling of sacrificial amorphous Si. Fig. 2 (a) illustrates the mock-up top-view of the proposed LWR in this work. Both top and bottom electrodes are based on molybdenum (Mo) with a thickness of 250 nm, a 1 µm thick layer of AlN is sandwiched between two electrodes. An addition 1 µm thick layer of AlCu serves as both routings and contact pads to reduce series resistance of the device. Fig. 2 (b) depicts the cross-sectional view of the LWR where the release cavity was defined within the interposer dielectric with a thickness of around 800 nm. Through this approach, the release region is well-defined and thus offers better acoustic energy confinement for attaining high Q resonator performance.

Lateral field excitation (LFE) is used to excite the proposed S_0 LWR. In this configuration. The top electrode of the LWR was made of interdigital transducers (IDT) while the bottom electrode is a metal plate at floating potential. Alternating voltage and ground potentials are being applied throughout the IDT structure, forming a mostly vertical electric field owing to the thin piezoelectric layer. Lateral stress was then induced through the piezoelectric constant e_{31}, forming a mode shape shown in Fig.3. Therefore, resonance can be excited simply by applying AC voltage signal to the MEMS device.

The phase velocity is first analyzed through investigating the dispersion behavior of S_0 wave propagating in the Mo-AlN-Mo stacking. The FEM simulation based on COMSOL Multiphysics [9] is depicted in Fig. 3(a). All the LWRs implemented in this work were designed at h_{AlN}/λ ratio < 0.1 to harvest the high phase velocity region of the S_0 mode. Furthermore, in this region the phase velocity of S_0-mode Lamb wave tends to stay rather constant, therefore making wavelength (or IDT pitch) the controlling factor determining the LWR frequency (as depicted in the phase velocity dispersion curve (Fig. 3 (a)), assuming a thickness-to-wavelength (h/λ) lower than 0.1). Therefore, by approximating the phase velocity into a constant value, the resonance frequency of the S_0 LWR designed at this h_{AlN}/λ range can be estimated through the follow equation:

$$f_r = \frac{v_p}{\lambda} = \frac{v_p}{2p} \quad (1)$$

v_p denotes the phase velocity of S_0 wave, λ is the wavelength, and p is the electrode pitch. Hence, through Eq. 1 it is noticed that λ is the key controlling factor for the LWR frequency. The frequency of the LWR can be scaled simply by defining a finer electrode pitch. To evaluate the electromechanical coupling of the S_0 LWR, the definition for k_{eff}^2 is based on the definition mentioned in [10][11]:

Which can then be expressed as:

$$k_{\mathrm{eff}}^2 = \frac{\pi^2}{8} \times \left(\frac{f_p^2 - f_s^2}{f_s^2}\right) \quad (2)$$

The 2D full model finite-element analysis (FEA) based on one resonator design (λ=12.4 µm with 9 electrode pairs and aperture of 12λ) was carried out [Fig. 2(b)], which depicts a series resonant frequency (f_s) of 713 MHz and a k_{eff}^2 of 1.04% with a given simulative Q-factor (Q_{sim}) of 2000.

MEASUREMENT SETUP AND RESULTS

Resonator performance characterization

The fabricated one-port S_0 LWR was measured in a RF probe station using GSG probes. Admittance response (Y-parameters) were obtained by conversion of scattering parameters (S-parameters) characterized in a Keysight E5071C vector network analyzer (VNA). All data was measured in a dry ambient condition with a typical driving RF power set to -10 dBm. In Fig. 4, the measured admittance response based on a S_0 LWR with wavelength of 12.4 µm is reported, exhibiting a high Q factor (Q_{fitted}) of 2,100 and k_{eff}^2 of 1.05%, which agreed well with our prediction based on properly predefined acoustic boundaries. The Q_{fitted} and k_{eff}^2 reported were based on a fitted multi-branch modified Butterworth van-Dyke (mBVD) model

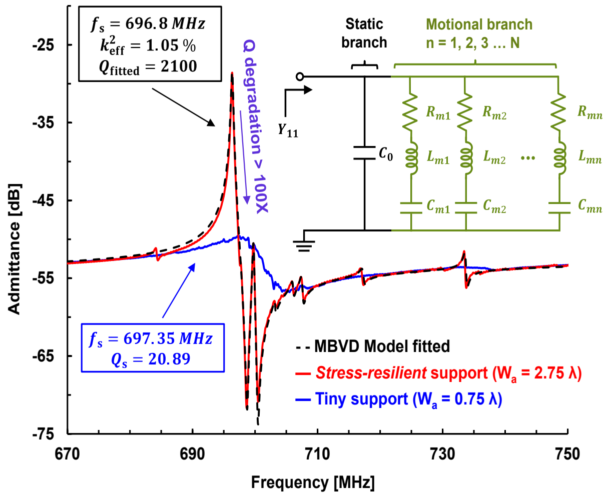

Figure 4. Measured admittance of fabricated S₀ LWRs with different resonator geomertie. A subplot is included to indicate the multi-branch MBVD model used to fit the admittance response.

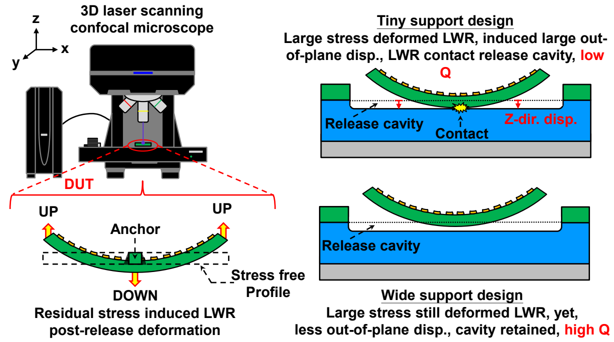

Figure 5. Measurement setup for the optical LWR deformation profile using the laser confocal microscopy and the inference of the contact-based failure mode.

as shown in the subplot of Fig. 4. The resonator is modeled based on the same multi-branch architecture introduced in [10] and contains n motional branches to include all spurious over the spectrum. However, comparing two similar S_0 LWRs with same wavelength (12.4 µm) and equal transducer capacitance (C_0) of 480 fF (as shown in Fig. 4) in terms of their admittance response. There existed a 100X quality factor degradation across LWR with wider anchor (W_a = 2.75λ, Q = 2100) and LWR with narrow anchor design (W_a = 0.75λ, Q = 21). The results present an unexpected low Q and exhibit an unusual trend as compared to previous research [12].

Optical surface profile measurement

To understand such a dramatic performance deviation, a 3-dimensional (3D) laser scanning confocal microscopy (Keyence VK-X series) is introduced for characterizing the surface profile of the LWRs, as shown in Fig. 5. Since it is speculated that such a large performance deviation between similarly sized devices is caused by the residual stress-induced physical contact between the resonator plate and the bottom of the cavity. The surface profile of multiple devices was captured and analyzed. As wider anchors offer higher mechanical stiffness, the out-of-plane deformation can be effectively suppressed to avoid contact while attain high-Q operation.

Fig. 6 depicts a comparison between three selected resonator types on the same wafer. LWR-A and LWR-C features similar geometry aspect ratio (W/L) of around 0.5 while LWR-B possess larger W/L of 1.33. It is noted that in our design, one of the plate dimensions in each resonator is fixed around 115µm, and the anchor width of LWR-C is 3.6X larger than LWR-A and LWR-B. By comparing the measured surface profile and the admittance response in Fig. 6, we can confirm that the decisive factor of Q in this platform being the amount of out-of-plane deformation (Δd) instead of aspect ratio or anchor size. As shown in Fig. 5(a), LWR-A devices exhibits a very low Q < 100 phenomenon as the Δd approaches the depth of the release cavity ($t_{\text{cavity}} \approx$ 800 nm), which indicates a physical contact between the bottom of the LWR and the bottom of the cavity. Furthermore, by observing LWR-B devices, it showed that even if Δd is smaller than t_{cavity}, excessive proximity between the LWR and the interposer dielectric can still lead to significant performance degradation [Fig. 6(b), Q = 263.23, $\Delta d \approx$ 670 nm]. As a result, a wide support design that can provide sufficient mechanical stiffness to sustain the post-release deformation [in Fig. 6(c)] becomes an effective and simple stress resilience solution to attain high of over Q > 2,400 for devices adapting sandbox-type shallow release cavities.

In addition to the out-of-plane deformation caused by residual stress, the stress curving of the LWR may also affect the performance. However, further investigation into the statistics in our measurement results depicted that the radius of curvature (R.O.C) of the deformed LWR along the wave propagation direction seems to have less effect on the overall Q factor. For instance, among the three types of LWR presented, the LWR-C devices feature highest Q factor despite having largest stress curving. Conversely, the Q factor of LWR-B devices are still 10X smaller than LWR-C devices even though stress curvature exhibit the least effect. Showing the less related correlation between device curvature and Q factor. Statistically, out of the 90 LWR-A type low Q (< 100) devices measured, 19 of which had their surface profile further captured using laser confocal microscopy and the results indicates a 100% correlation between low Q and out-of-plane deformation around 800 nm. Which further consolidates our speculation about the new failure mode for LWR based this type of shallow release cavities. Which is mostly caused by the boundary condition change due to the physical contact between LWR and release cavity.

CONCLUSIONS

In conclusion, a UHF S_0 LWR with both high Q factor of over 2400 and k_{eff}^2 more than 1% was reported in this work. The precisely defined acoustic boundary can both provide good acoustic energy confinement and maintain good structural robustness. By utilizing the "release sandbox" concept, the unwanted undercut during substate isotropic release was completely removed. Therefore, an overall f-Q product of over 1.6 × 10^{12} can be achieved. However, devices exhibiting abnormally low Q were also discovered during our performance characterization. By analyzing the measured device performance and its corresponding surface profile, a new mode of failure for LWR based on shallow release cavity is identified. Concluding that although tiny support has long been proven to provide less anchor loss and higher Q, maintaining sufficient mechanical stiffness to withstand the residual stress deformation can be an alternative if increasing cavity depth is not feasible. By avoiding contact between LWR and cavity. the ideal boundary condition for a high Q LWR device can still be maintained even in a shallow release cavity.

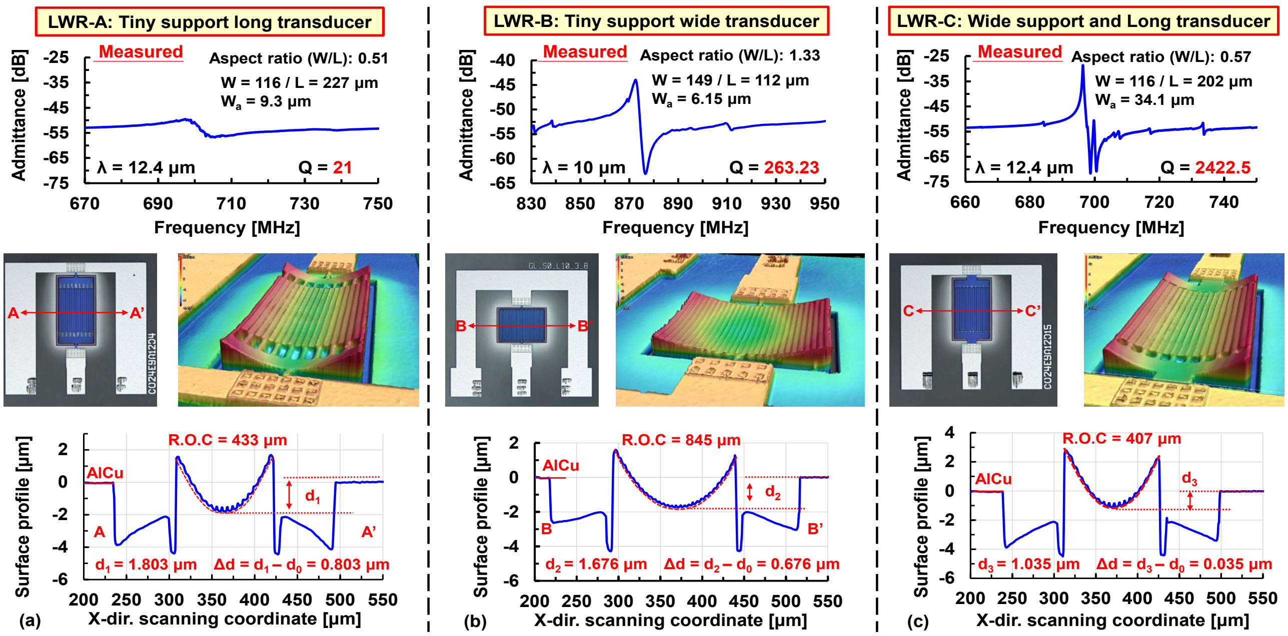

Figure 6. Measurement data across three transducer designs: (a) tiny support with small transducer aspect ratio (LWR-A); (b) tiny support with large transducer aspect ratio (LWR-B); (c) wide support with small transducer aspect ratio (LWR-C). All profile measurements were referenced to the top surface of the AlCu layer and the 3D profile images were rendered with a 400X magnification.

ACKNOWLEDGEMENTS

The author would like to acknowledge Vanguard International Semiconductor Corporation for the device fabrication, and the Taiwan Semiconductor Research Institute (TSRI) for the assistance and measurement facility during device performance acquisition. This work was partially supported by the Ministry of Science and Technology (MOST) of Taiwan under Grant MOST 110-2636-E-007-012 (Young Scholar Fellowship Program).

REFERENCES

[1] S. Mahon and R. Aigner, "Bulk Acoustic Wave Devices – Why, How, and Where They are Going," in *Proc.* CS MANTECH Conference, pp. 15-18, Austin, Texas, USA, May 2007

[2] V. Yantchev and I. Katardjiev, "Thin film Lamb wave resonators in frequency control and sensing applications: a review," *J. Micromech. Microeng.*, vol. 23, pp. 043001, Mar. 2013.

[3] C.-M. Lin, V. Yantchev, J. Zou, Y.-Y. Chen, and A. P. Pisano, "Micromachined One-Port Aluminum Nitride Lamb Wave Resonators Utilizing the Lowest-Order Symmetric Mode," *J. Microelectromech. Syst.*, vol. 23, pp. 78-91, Feb. 2014.

[4] B. Gibson, K. Qalandar, C. Cassella, G. Piazza and K. L. Foster, "A Study on the Effects of Release Area on the Quality Factor of Contour-Mode Resonators by Laser Doppler Vibrometry," *IEEE Trans. Ultrason., Ferroelectr., Freq. Control*, vol. 64, no. 5, pp. 898-904, May 2017.

[5] A. Gao, M. Winterkorn, Y. Yang, R. Lu, J. Provine and S. Gong, "Boosting Qs of AlN Resonators by Redefining Acoustic Boundaries," in *Proc.* IEEE 32nd Int. Conf. Micro Electro Mech. Syst. (MEMS), pp. 883-886, Seoul, Korea (South), Jan. 2019.

[6] H. Campanella, Y. Qian, C. O. Romero, J. S. Wong, J. Giner and R. Kumar, "Monolithic Multiband MEMS RF Front-End Module for 5G Mobile," *J. Microelectromech. Syst.*, vol. 30, no. 1, pp. 72-80, Feb. 2021.

[7] A. Lozzi, A. De Pastina, L. G. Villanueva and E. T. Yen, "Release area confinement in contour mode resonators," in *Proc.* IEEE International Ultrasonics Symposium (IUS), pp. 1-4, Washington, DC, USA, Sep. 2017.

[8] https://www.comsol.ch/

[9] T. Yokoyama, Y. Iwazaki, T. Nishihara and J. Tsutsumi, "Dopant concentration dependence of electromechanical coupling coefficients of co-doped AlN thin films for BAW devices," in *Proc.* IEEE International Ultrasonics Symposium (IUS), pp. 1-4, Tours, France, Sep. 2016.

[10] R. Lu, M.-H. Li, Y. Yang, T. Manzaneque and S. Gong, "Accurate Extraction of Large Electromechanical Coupling in Piezoelectric MEMS Resonators," *J. Microelectromech. Syst.*, vol. 28, no. 2, pp. 209-218, April 2019.

[11] C. Cassella, N. Oliva, J. Soon, M. Srinivas, N. Singh and G. Piazza, "Super High Frequency Aluminum Nitride Two-Dimensional-Mode Resonators With k_t^2 Exceeding 4.9%," *IEEE Microwave and Wireless Components Letters*, vol. 27, no. 2, pp. 105-107, Feb. 2017.

[12] J. Segovia-Fernandez, M. Cremonesi, C. Cassella, and G. Piazza, "Anchor Losses in AlN Contour Mode Resonators," *J. Microelectromech. Syst.* vol. 24. no. 2. pp.265-275, Apr. 2015.

CONTACT

*Ming-Huang Li; mhli@pme.nthu.edu.tw